Journal of Crystal Growth 311 (2009) 4447–4453

Contents lists available at ScienceDirect

Journal of Crystal Growth

journal homepage: www.elsevier.com/locate/jcrysgro

Effect of solid–liquid density change on dendrite tip velocity and shape selection

Y. Sun [a], C. Beckermann [b,*]

[a] Department of Mechanical Engineering, State University of New York at Binghamton, Binghamton, NY 13902, USA
[b] Department of Mechanical and Industrial Engineering, The University of Iowa, Iowa City, IA 52242, USA

ARTICLE INFO

Article history:
Received 22 January 2009
Received in revised form
10 July 2009
Accepted 27 July 2009
Communicated by J.J. Derby
Available online 6 August 2009

PACS:
47.11.−j
68.70.+w
81.30.Fb

Keywords:
A1. Density difference
A1. Phase-field method
A1. Shrinkage flow
A1. Solidification
A2. Dendritic growth

ABSTRACT

Phase-field simulations are used to examine tip velocity and shape selection in free dendritic growth of a pure substance into an undercooled melt in the presence of a density change between the solid and liquid. The dendrite is assumed to grow two-dimensionally inside a Hele-Shaw cell. The phase-field model is coupled with a previously developed two-phase diffuse interface model to simulate the flow in the liquid that is induced by the density change. The predicted dependence of the dendrite tip growth Péclet number on the relative density change is compared with an available analytical solution and good agreement is obtained. The simulations verify that the dendrite tip selection parameter, modified to account for the different densities of the solid and liquid phases, is independent of the relative density change.

1. Introduction

Dendritic growth is of fundamental importance in the solidification of many materials. Usually, such crystal growth involves a density change between the solid and liquid phases. This density change induces a contraction or expansion flow in the undercooled melt ahead of the dendrite. McFadden and Coriell [1], for an axisymmetric paraboloidal dendrite, and Emmerich [2], for a two-dimensional parabolic plate dendrite, extended the Ivantsov solution for free dendritic growth of a pure substance into an undercooled melt to include the effects of a density change upon solidification. In the extended Ivantsov solution, the tip growth Péclet number, Pe, is a function not only of the imposed dimensionless melt undercooling, Δ, but also of the relative density change, β. The relative density change is defined as $\beta = \rho_s/\rho_l - 1$, where ρ_s and ρ_l are the densities of the solid and liquid, respectively. From the solution of the Navier–Stokes equation, the magnitude of the flow in the melt was found to be of the order of β, with the velocity decaying to zero with increasing distance from the dendrite. Despite the fact that the density change induced flow plays an important role, the extended Ivantsov solution does not contain the Prandtl number or, more directly, the liquid viscosity. This result is different from the case of dendritic growth with forced convection in the melt, where the growth Péclet number depends also on the Prandtl number [3].

Emmerich [2] also modified the microscopic solvability theory of Kessler et al. [4] for dendrite tip velocity and shape selection to include the effects of a density change. According to this theory, a unique dendrite tip velocity and shape is selected by the action of anisotropic surface tension via a selection parameter σ^*, and at low undercoolings, σ^* is a constant that only depends on the crystalline anisotropy strength ε. In the presence of a density change, Emmerich [2] found that the relation for the selection parameter must be modified to include the relative density change. With this modification, σ^* should take the same value as for diffusion limited dendritic growth without a density change. To date, this theory has not been validated by either experiments or direct numerical simulations.

In recent years, phase-field methods and other diffuse interface approaches have been popular tools in the direct numerical simulation of dendritic growth from the melt [5,6]. By introducing an order parameter, ϕ, to represent the transition between the

* Corresponding author. Tel.:+1 319 335 5681; fax: +1 319 335 5669
E-mail address: becker@engineering.uiowa.edu (C. Beckermann).

0022-0248/$ - see front matter © 2009 Elsevier B.V. All rights reserved.
doi:10.1016/j.jcrysgro.2009.07.031

solid and liquid, a unique set of evolution equations is solved over the entire domain without explicitly tracking the solid–liquid interface. Due to the strong influence of melt motion on the evolution of microstructures during solidification, efforts have been made to include convection within phase-field models [7–10]. For the sake of simplicity, most phase-field simulations of solidification assume equal densities in the solid and liquid. Recently, several phase-field simulations [2,11–16] have been carried out that account for the density change induced flow during free dendritic growth. Although these studies have revealed much interesting physics, it is not always clear if the results correspond to the same sharp interface model for which analytical solutions were obtained previously and/or if the results are fully converged with respect to the width of the diffuse interface. None of the previous studies have examined the effect of the density change on the dendrite tip selection parameter, σ^*.

In this paper, the phase-field model of Karma and Rappel [17] is used in junction with the two-phase diffuse interface approach of Sun and Beckermann [18,19] to examine tip velocity and shape selection in two-dimensional free dendritic growth of a pure substance into an undercooled melt in the presence of a density change. The remainder of this paper is organized as follows. In Section 2, an available theory for two-dimensional (2D) dendritic growth with density change is reviewed. A sharp interface description of the problem being solved is provided in Section 3. The corresponding phase-field model is summarized in Section 4. Section 5 describes the numerical procedure used to solve the model equations. The results and conclusions are presented in Sections 6 and 7, respectively.

2. Theory of 2D dendritic growth with density change

The basic theory of free dendritic growth predicts the steady-state tip velocity, V, and tip radius of curvature, R, of a dendritic needle crystal of a pure substance growing into an infinite undercooled melt. For a two-dimensional parabolic plate dendrite, and equal densities of the solid and liquid, the analytical solution of the heat equation for diffusion limited growth is given by

$$\Delta = Iv_2(Pe) \tag{1}$$

where $\Delta = (T_m - T_\infty)/(L/c_p)$ is the dimensionless melt undercooling, T_m and T_∞ are the equilibrium melting temperature and the far-field temperature, respectively, L is the latent heat of fusion, and c_p is the specific heat. The dendrite tip growth Péclet number is defined as $Pe = VR/(2\alpha_l)$, where α_l is the liquid thermal diffusivity. The Ivantsov function for a two-dimensional plate dendrite, $Iv_2(x)$, is given by

$$Iv_2(x) = \sqrt{\pi x}\exp(x)erfc(\sqrt{x}) \tag{2}$$

where $erfc(x)$ is the complementary error function. In the presence of density change flow, Emmerich [2] obtained the following extended Ivantsov solution,

$$\Delta(\beta) = (1+\beta)\sqrt{\pi Pe}\exp[Pe(1+\beta)^2]erfc[\sqrt{Pe}(1+\beta)] \tag{3}$$

where β is the relative density change, as defined in the Introduction. Eq. (3) implies that the effect of the density change on the heat transfer rate at the dendrite tip is of the order of β. The corresponding extended Ivantsov solution for an axisymmetric dendrite can be found in McFadden and Coriell [1].

According to microscopic solvability theory [4], a unique dendrite tip velocity is selected by the action of anisotropic surface tension via the scaling relation

$$\sigma^* = \frac{2\alpha_l d_0}{R^2 V} \tag{4}$$

where d_0 is the thermal capillary length. The selection parameter σ^* is a constant that only depends on the anisotropy strength ε as $\sigma^* \sim \varepsilon^{1.75}$ in the limit of small ε. Emmerich [2] extended the solvability theory to include the density change between the solid and liquid phases and derived the following modified selection equation

$$\sigma^* = \frac{2\alpha_l d_0}{R^2 V(1+\beta)} = \frac{d_0}{RPe(1+\beta)} \tag{5}$$

The main motivation of the present study is to verify, by direct numerical simulation, the theory of Emmerich [2] that the selection parameter σ^*, as defined by Eq. (5), is not a function of the relative density change, β, and takes the same value as for equal densities.

3. Sharp interface description

Before presenting the present phase-field model, it is important to state the conventional sharp interface equations for the dendritic growth problem being solved. In order to reduce computational effort, the growth is assumed to take place inside of a horizontal Hele-Shaw cell with a narrow gap of width b that is much smaller than the cell dimension L (i.e., $b \ll L$). This assumption renders the problem two-dimensional. Due to the small gap width, inertia effects can be neglected so that the density change induced flow in the liquid is purely viscous. While the densities of the solid and liquid are taken to be unequal (but constant), the thermal conductivities (k) and specific heats (c_p) of the solid and liquid are assumed to be equal. Solid–liquid interface kinetic effects and the Clausius–Clapeyron effect (i.e., the dependence of the melting temperature on pressure) are neglected. The gap-averaged sharp interface equations can then be written as

Liquid:

$$\nabla \cdot \boldsymbol{u}_l = 0 \quad \text{(continuity)} \tag{6}$$

$$\boldsymbol{u}_l = -\frac{b^2}{12\mu_l}\nabla p_l \quad \text{(momentum)} \tag{7}$$

$$\frac{\partial \theta}{\partial t} + \boldsymbol{u}_l \cdot \nabla\theta = (1+\beta)\alpha_s \nabla^2\theta \quad \text{(energy)} \tag{8}$$

Solid:

$$\frac{\partial \theta}{\partial t} = \alpha_s \nabla^2 \theta \quad \text{(energy)} \tag{9}$$

Interface:

$$\boldsymbol{u}_l \cdot \boldsymbol{n} = -\beta \boldsymbol{u}_i \cdot \boldsymbol{n} \quad \text{(continuity)} \tag{10}$$

$$\boldsymbol{u}_i \cdot \boldsymbol{n} = \alpha_s \left(\left.\frac{\partial\theta}{\partial n}\right|_s - \left.\frac{\partial\theta}{\partial n}\right|_l \right) \quad \text{(Stefan condition)} \tag{11}$$

$$\theta = -d_0(1 - 15\varepsilon\cos 4\varphi)\kappa \quad \text{(Gibbs}-\text{Thomson condition)} \tag{12}$$

where $\boldsymbol{u}_l$ is the liquid velocity, μ_l the liquid dynamic viscosity, p_l the liquid pressure, $\boldsymbol{u}_i$ the interface velocity, $\theta=(T-T_m)/(L/c_p)$ the dimensionless temperature, ε the fourfold anisotropy strength, $\boldsymbol{n}$ the interface unit normal vector pointing outward of the solid phase, φ the angle of the interface normal vector, and κ the interface curvature. The thermal capillary length is defined as $d_0=\sigma T_m c_p/\rho_s L^2$, where σ is the interfacial tension between the solid and liquid. Note that the above equations are written in terms of the thermal diffusivity of the solid, which is given by $\alpha_s=k/(c_P\rho_s)=\alpha_l/(1+\beta)$. This was done only to make the above sharp interface equations correspond more directly to the phase-field model presented in the next section.

4. Phase-field model

Based on the two-phase diffuse interface model for Hele-Shaw flow recently developed by Sun and Beckermann [19], the continuity equation can be written in a dimensionless form as

$$\nabla'\cdot[(1-\phi)\boldsymbol{u}'_l]=-\beta\frac{\partial\phi}{\partial t'} \tag{13}$$

where the phase-field ϕ varies from unity in the solid phase to zero in the liquid over a distance of approximately $3\sqrt{2}W_0$, where W_0 is a measure of the diffuse interface width. The other dimensionless variables are defined as $\boldsymbol{u}'_l=\boldsymbol{u}_l\tau_0/W_0$, $\nabla'=\nabla W_0$, and $t'=t/\tau_0$, where τ_0 is the relaxation time. Based on the Hele-Shaw approximation, the dimensionless momentum equation for the present diffuse interface model is given by [19]

$$\boldsymbol{u}'_l=-\frac{b'^2}{12}\left[\nabla' p'_l-\frac{\sigma'\phi}{\sqrt{2}}\nabla'\left(\frac{\nabla'^2\phi}{\phi(1-\phi)}\right)\right] \tag{14}$$

where $b'=b/W_0$, $p'_l=p_l\tau_0/\mu_l$, and $\sigma'=\sigma\tau_0/(\mu_l W_0)$. The second term inside the square brackets of Eq. (14) is a capillary stress gradient term that is non-zero only inside the diffuse interface. The reader is referred to Sun and Beckermann [18,19] for a detailed discussion of this term and its effect on the variation of the pressure inside the diffuse interface. The diffuse interface energy conservation equation can be derived using the same averaging methods as in Sun and Beckermann [18], and the result is given by

$$\left(\phi+\frac{1-\phi}{1+\beta}\right)\frac{\partial\theta}{\partial t'}+\frac{1}{1+\beta}\boldsymbol{u}'_l(1-\phi)\cdot\nabla'\theta=\tilde{\alpha}\nabla'^2\theta+\frac{\partial\phi}{\partial t'} \tag{15}$$

where the dimensionless thermal diffusivity is given by $\tilde{\alpha}=\alpha_s\tau_0/W_0^2$.

Since the solid is assumed to be stationary and the effect of pressure on the interface temperature is neglected, the phase-field equation is identical to the one derived by Karma and Rappel [5] for dendritic growth under purely diffusive conditions

$$\begin{aligned}(1+\varepsilon\cos 4\varphi)^2\frac{\partial\psi}{\partial t'}=&\nabla'^2\psi+\psi(1-\psi^2)-\lambda(1-\psi^2)^2\theta\\&+\varepsilon\cos 4\varphi(2+\varepsilon\cos 4\varphi)\nabla'^2\psi\\&-8\varepsilon\sin 4\varphi(1+\varepsilon\cos 4\varphi)(\varphi_x\psi_x+\varphi_y\psi_y)\\&-16\varepsilon[\cos 4\varphi+\varepsilon(\cos^2 4\varphi-\sin^2 4\varphi)]\\&(\varphi_y\psi_x-\varphi_x\psi_y)\end{aligned} \tag{16}$$

where ψ is a modified phase-field given by $\psi=2\phi-1$. The modified phase-field varies smoothly from 1 in the solid to -1 in the liquid over a small but numerically resolvable diffuse interface region, and the solid–liquid interface is defined by the contour $\psi=0$. The angle between the direction normal to the interface and the horizontal axis is calculated from the phase-field via $\varphi=\arctan(\partial_y\psi/\partial_x\psi)$. Eq. (16) is non-dimensionalized using τ_0 and W_0, and λ is the so-called coupling constant. The relations $W_0=\lambda d_0/a_1$ and $\tau_0=(d_0^2/\alpha_s)a_2\lambda^3/a_1^2$ follow from the thin-interface analysis of Karma and Rappel [5], where a_1 and a_2 are constants. The coupling constant λ is the only free parameter and the results should be independent of λ once they are converged. Decreasing λ corresponds to decreasing the diffuse interface width, since $\lambda=a_1W_0/d_0$.

5. Numerical procedures

The model described in the preceding section is used to numerically simulate the growth of a two-dimensional dendrite with flow induced by a density difference between the solid and liquid. The simulation domain is schematically illustrated in Fig. 1. Taking advantage of symmetry, only one quadrant of a dendrite is computed; thus the initial seed is actually only a quarter of a circle. The crystal axes are aligned with the coordinate axes. Symmetry boundary conditions are applied for all fields on the left and bottom boundaries. The pressure is assumed to be constant on the upper and right boundaries. The initial dimensionless melt temperature is set to be $-\Delta$ (undercooling), except inside the seed where the dimensionless temperature is set to zero.

The continuity and momentum equations for the flow are solved numerically using a conjugate-gradient pressure Poisson solver on a uniform mesh. The phase-field and energy equations are solved using an explicit Euler scheme. The flow is only calculated every 10 time steps used in the phase-field and energy equation solution [20]. The advection term in the energy equation is discretized using a fourth-order convex essentially non-oscillatory (CENO) scheme.

Due to anisotropy, the circular seed grows preferentially along the horizontal and vertical axes, developing arms as shown in Fig. 2. The rate of change of the tip position of these arms is defined as the tip velocity. The radius of curvature of the tip is calculated using the same method as in Ramirez and Beckermann [21]. When the tip velocity and radius of curvature cease to change with time, the steady-state growth regime is achieved for which the analytical solution of Emmerich [2] is valid. Based on experience from previous studies [20–22], the dimensionless grid spacing is set to $\Delta x=0.8$, the dimensionless time step to

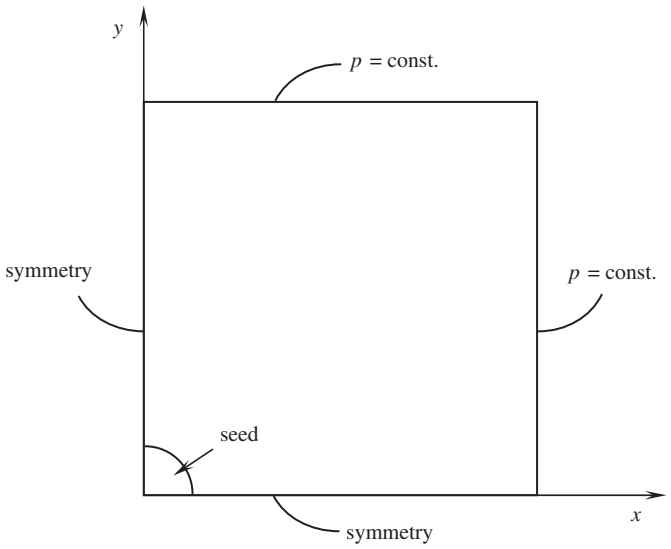

Fig. 1. Phase-field simulation domain and boundary conditions.

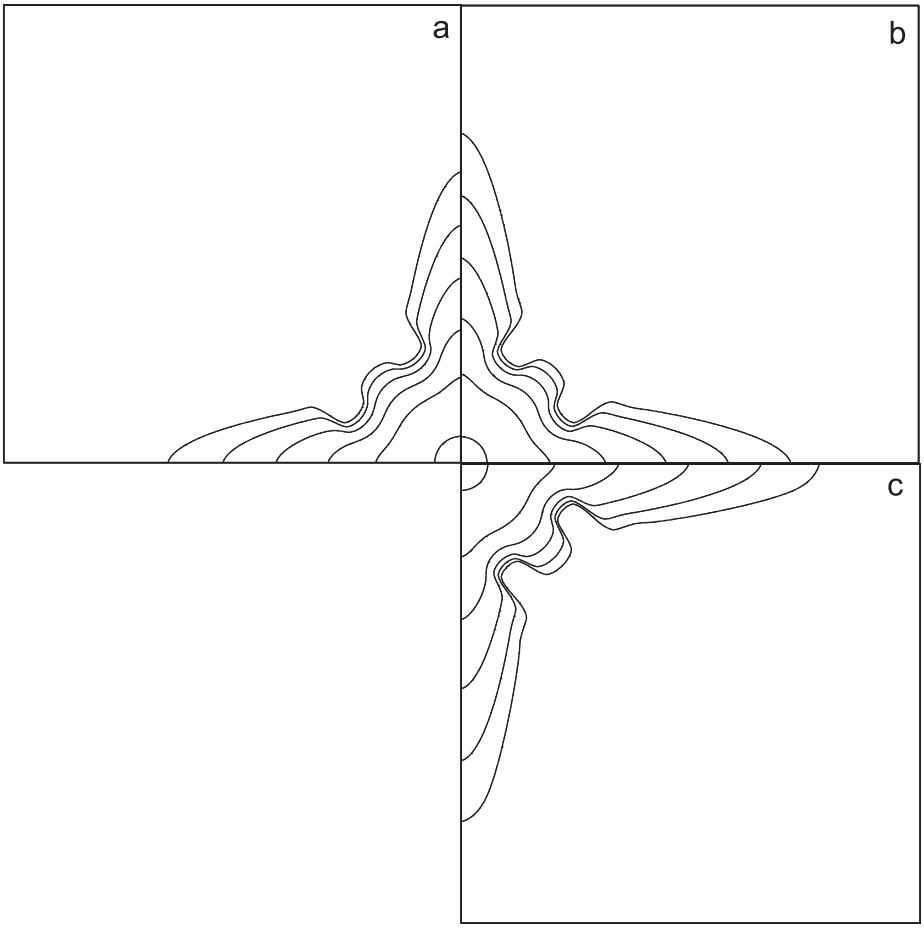

Fig. 2. Evolution of phase-field contours, every 100,000 time steps, for a dendrite growing at $\Delta = 0.55$ and $\varepsilon = 0.05$ for (a) $\beta = 0.1$, (b) $\beta = 0$ (no flow), and (c) $\beta = -0.1$.

$\Delta t = 0.018$, and the coupling constant, λ, that dictates the interface width to $\lambda = 4$. For equal densities of the solid and liquid, when the growth is under purely diffusive conditions, identical results to those of Karma and Rappel [5] and Tong et al. [20] were obtained. These references demonstrate that the above choices for the grid spacing, time step and diffuse interface width give reasonably well converged results. Convergence studies for the Hele-Shaw flow calculations can be found in Sun and Beckermann [19].

6. Results and discussion

All dendritic growth simulations in the present study were performed for a melt undercooling of $\Delta = 0.55$ and an anisotropy strength of $\varepsilon = 0.05$. Fig. 2 shows the predicted evolution of the phase-field contours ($\psi = 0$), every 100,000 time steps, for three different values of the relative density change: $\beta = 0.1$, $\beta = 0$, and $\beta = -0.1$. It can be seen that the growth of the dendrite is strongly affected by the density change. Compared to the equal density case (Fig. 2b), the dendrite grows slower when shrinkage occurs upon solidification, as shown in Fig. 2a for $\beta = 0.1$. In contrast, when $\beta = -0.1$, as shown in Fig. 2c, the growth velocity is faster than in the equal density case.

Fig. 3 shows the liquid velocity vectors and phase-field contours for two different relative density changes: $\beta = 0.1$ (shrinkage) and $\beta = -0.1$ (expansion). Fig. 3a provides results at $t\alpha_s/d_0^2 = 190{,}000$ and Fig. 3b at $t\alpha_s/d_0^2 = 380{,}000$. For $\beta = 0.1$, the liquid flows toward the solid–liquid interface to compensate for the shrinkage upon solidification. On the other hand, for $\beta = -0.1$, the liquid flows away from the solidification front, since the solid has a lower density than the liquid. In both cases, the flow velocity is the highest at the dendrite tips, as opposed to other parts of the solid–liquid interface, since the tips have the highest growth velocity [see Eq. (10)]. The flow velocity decreases continually with increasing distance from the dendrite. These findings agree with the results of McFadden and Coriell [1].

As already mentioned, the presence of shrinkage reduces the dendrite growth rate. This result may be somewhat unexpected, since the melt flows toward the dendrite. In the case of forced convection (but equal densities of the solid and liquid), a flow towards a dendrite tip increases its growth rate [20,23]. The increase in the growth rate in the forced convection case can be attributed to advection of undercooled liquid towards the dendrite, resulting in a thinner thermal boundary layer and higher temperature gradients at the solid–liquid interface. In order to clarify this issue, the steady-state temperature fields (at $t\alpha_s/d_0^2 = 380{,}000$) predicted for $\beta = 0.1$, $\beta = 0$, and $\beta = -0.1$ are compared in Fig. 4. It may be seen that the thermal boundary layer on the liquid side of the solid–liquid interface is the thickest in the case of shrinkage ($\beta = 0.1$, Fig. 4a), even though the flow advects undercooled liquid towards the dendrite. The thicker thermal boundary layer causes the dendrite to grow more slowly in the presence of shrinkage. The opposite is true in the case of expansion ($\beta = -0.1$, Fig. 4c). These differences in the thermal boundary layer thickness can be explained by the fact that the density change not only induces a flow in the liquid, but it also changes the thermal diffusivity. This can be most easily seen from

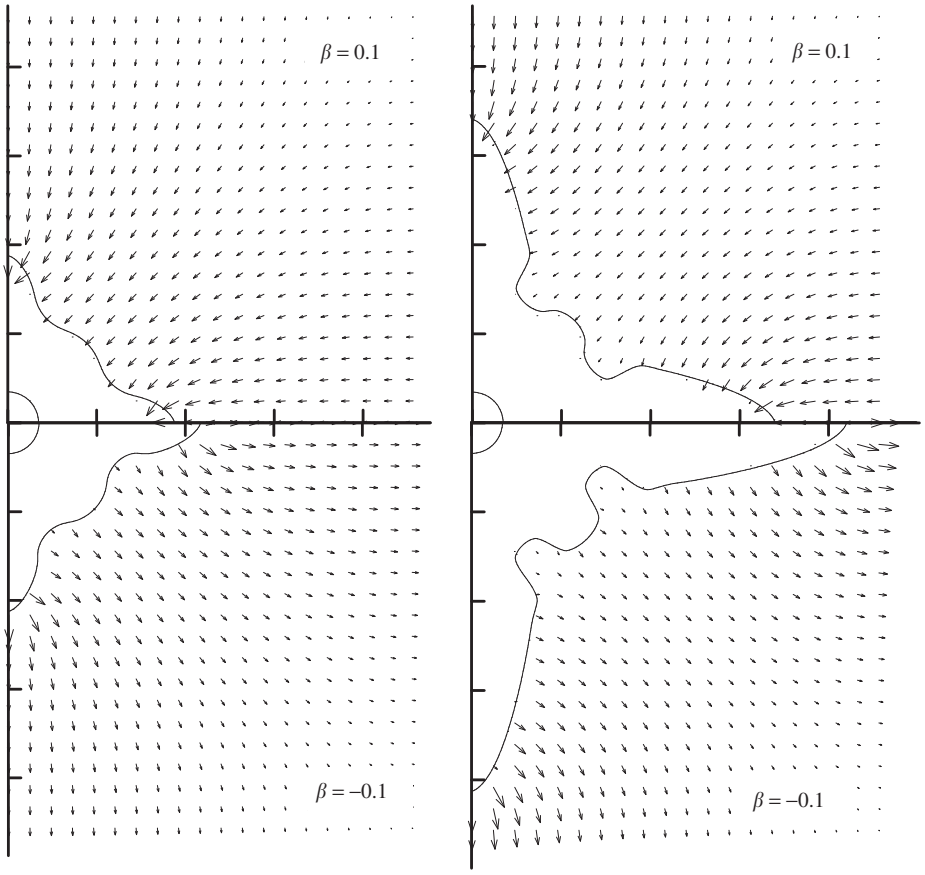

Fig. 3. Velocity vectors at (a) $t\alpha_s/d_0^2 = 190{,}000$ and (b) $t\alpha_s/d_0^2 = 380{,}000$ for a dendrite growing at $\Delta = 0.55$ and $\varepsilon = 0.05$; the upper two panels are for $\beta = 0.1$ (shrinkage) and the lower panels for $\beta = -0.1$ (expansion).

the energy equation for the liquid phase, Eq. (8). There is a factor of $(1+\beta)$ in front of the heat diffusion term on the right-hand-side of Eq. (8). Hence, for shrinkage ($\beta > 0$), heat diffusion in the liquid is enhanced, which results in a thicker thermal boundary layer and shallower temperature gradients along the solid–liquid interface. This effect is stronger than the advection of undercooled liquid towards the dendrite by the shrinkage-driven flow (which would reduce the thermal boundary thickness), resulting in the dendrite to grow more slowly. Again, the opposite is true for $\beta < 0$.

Fig. 5 shows predicted steady-state dendrite tip growth Péclet numbers as a function of the relative density change, β. Simulations were performed for five different β values, ranging from -0.1 to 0.1. It can be seen that the Péclet number decreases with an increasing relative density change. Fig. 5 also shows that the Péclet numbers predicted by the phase-field simulations are in good agreement with, but slightly above, the analytical solution given by Eq. (3). It should be noted that Emmerich [2] derived this solution for flow governed by the Navier–Stokes equations, rather than for Hele-Shaw flow. However, the solution given by Eq. (3) depends only on the flow normal to the dendrite tip, which has a dimensionless normal velocity component at the dendrite tip equal to βPe. For the Hele-Shaw flow considered here, the flow velocity normal to the interface is also equal to βPe. In other words, the type of flow and the liquid viscosity affect only the pressure field, and not the heat transport at the dendrite tip. Hence, the comparison shown in Fig. 5 is valid and the good agreement instills considerable confidence in the present numerical simulations.

Predicted dendrite tip selection parameters, σ^*, as a function of the relative density change, β, are shown in Fig. 6. The definition of σ^* given by Eq. (5) was used. It can be seen that σ^* is essentially constant and independent of the relative density change. For the range of relative density changes considered ($-0.1 \le \beta \le 0.1$), the selection parameter varies by less than 2%, which is well within the present numerical uncertainty. This finding constitutes the key result of the present study. It verifies that Emmerich's [2] definition of the selection parameter is appropriate for dendritic growth in the presence of a density change between the solid and liquid phases. If the traditional definition of the selection parameter given by Eq. (4) had been used instead, σ^* would have varied by 20%.

7. Conclusion

The effect of a density change between the solid and liquid phases on free dendritic growth of a pure material into an undercooled melt is examined using phase-field simulations. The dendritic growth is assumed to be two-dimensional and inside of a Hele-Shaw cell. Good agreement is obtained with the analytical solution of Emmerich [2] for the dependence of the dendrite tip growth Péclet number on the relative density change, β. The modified dendrite tip selection parameter σ^*, as defined by Emmerich [2], is found to be a constant that is independent of the relative density change. These results validate the available theory for dendritic growth in the presence of a density change. The density change should generally not be neglected when analyzing

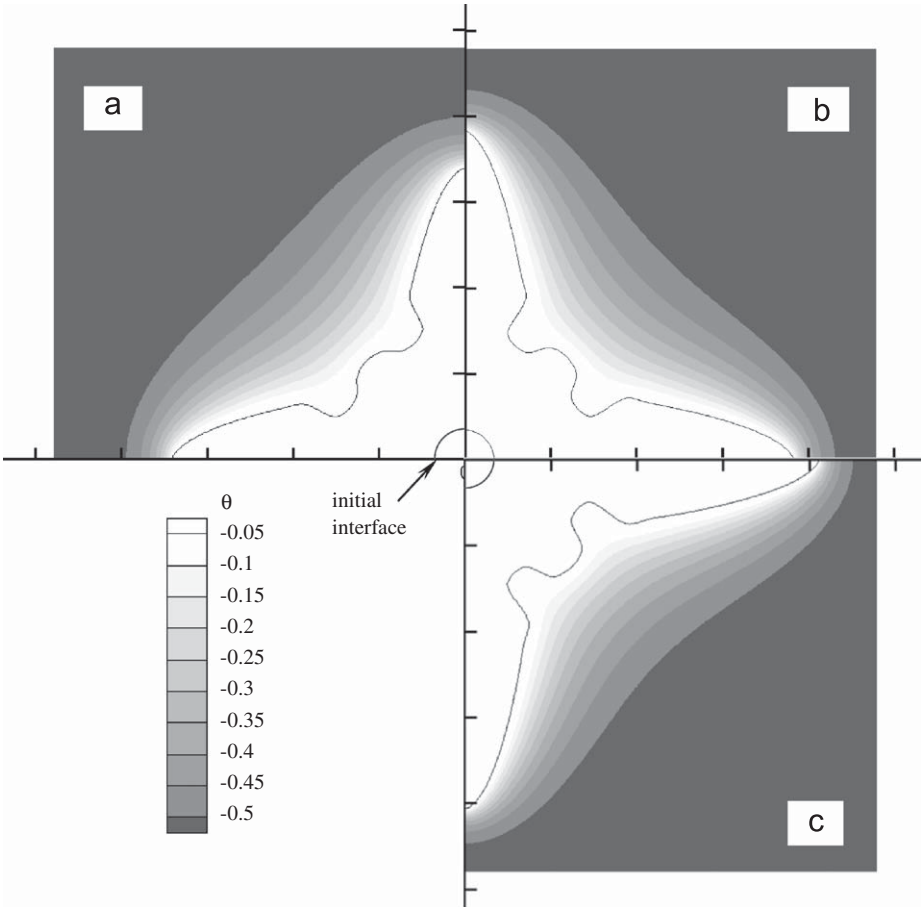

Fig. 4. Dimensionless temperature field (grey scale) and phase-field (black line) at $t\alpha_s/d_0^2 = 380{,}000$ for a dendrite growing at $\Delta = 0.55$ and $\varepsilon = 0.05$ for (a) $\beta = 0.1$, (b) $\beta = 0$, and (c) $\beta = -0.1$.

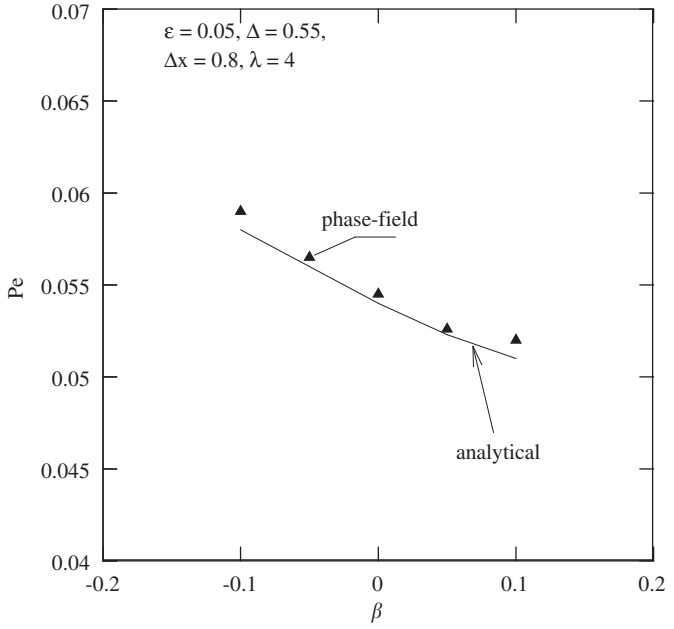

Fig. 5. Comparison between the dendrite tip growth Péclet number as a function of the relative density change from the phase-field simulations (symbols) and the analytical solution of Emmerich [2] (line).

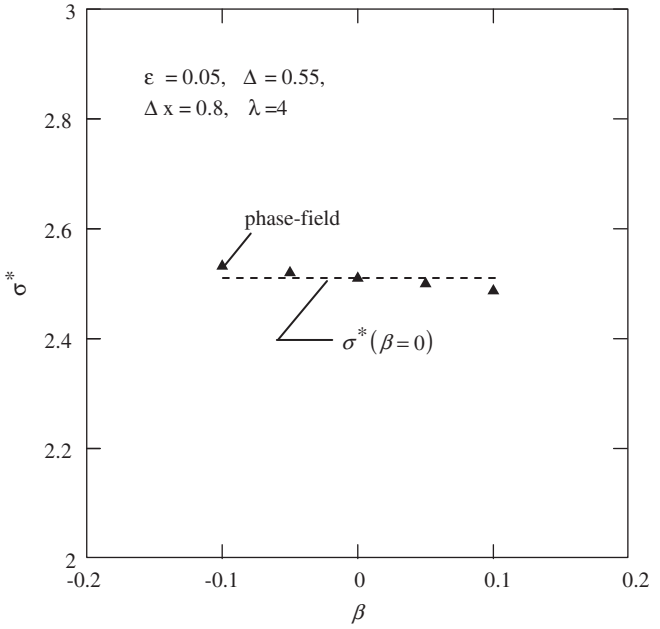

Fig. 6. Variation of the dendrite tip selection parameter from the phase-field simulations with the relative density change.

dendritic growth data. As pointed out by Emmerich [2], for a material such as succinonitrile, where the relative density change is only $\beta = 0.028$, the dendrite tip velocity is reduced by about 5% relative to the equal density case. Future work should include an investigation of the effects of different specific heats and thermal conductivities between the solid and liquid phases on dendritic growth, since those differences can be significant as well.

Acknowledgement

This work was supported in part by the US National Science Foundation under Grant no. DMR-0132225.

References

[1] G.B. McFadden, S.R. Coriell, The effect of fluid flow due to the crystal-melt density change on the growth of a parabolic isothermal dendrite, J. Cryst. Growth 7 (1986) 507–512.
[2] H. Emmerich, The Diffuse Interface Approach in Materials Science: Thermodynamics Concepts and Applications of Phase-Field Models, Lecture Notes in Physics M73, Springer, Heidelberg, 2003.
[3] S.K. Dash, W.N. Gill, Forced-convection heat and momentum-transfer to dendritic structures (parabolic cylinders and paraboloids of revolution), J. Heat Mass Transfer 27 (1984) 1345–1356.
[4] D. Kessler, J. Koplik, H. Levine, Pattern selection in fingered growth phenomena, Adv. Phys. 37 (1988) 255–339.
[5] A. Karma, W.-J. Rappel, Quantitative phase-field modeling of dendritic growth in two and three dimensions, Phys. Rev. E 57 (1998) 4323–4349.
[6] W.J. Boettinger, J.A. Warren, C. Beckermann, A. Karma, Phase-field simulation of solidification, Annu. Rev. Mater. Res. 32 (2002) 163–194.
[7] C. Beckermann, H.J. Diepers, I. Steinbach, A. Karma, X. Tong, Modeling melt convection in phase-field simulations of solidification, J. Comput. Phys. 154 (1999) 468–496.
[8] R. Tönhardt, G. Amberg, Simulation of natural convection effects on succinonitrile crystals, Phys. Rev. E 62 (2000) 828–836.
[9] D.M. Anderson, G.B. McFadden, A.A. Wheeler, A phase-field model of solidification with convection, Physica D 135 (2000) 175–194.
[10] D.M. Anderson, G.B. McFadden, A.A. Wheeler, A sharp-interface analysis of solidification with convection, Physica D 151 (2001) 305–331.
[11] D.M. Anderson, G.B. McFadden, A.A. Wheeler, A phase-field model of solidification with convection: numerical simulations, in: M.K. Smith et al.(Ed.), Interfaces for the Twenty-First Century, Imperial College Press, 2002, pp. 131–145.
[12] D.M. Anderson, G.B. McFadden, and A.A. Wheeler, A phase-field model of convection with solidification, 40th AIAA Aerospace Sciences Meeting & Exhibit, Reno, NV, (2002) AIAA Paper no. 2002-0891.
[13] M. Conti, Density change effects on crystal growth from the melt, Phys. Rev. E 64 (2001) 051601.
[14] M. Conti, M. Fermani, Interface dynamics and solute trapping in alloy solidification with density change, Phys. Rev. E 67 (2003) 026117.
[15] M. Conti, Advection flow effects in the growth of a free dendrite, Phys. Rev. E 69 (2004) 022601.
[16] J. Narski, M. Picasso, Adaptive 3D finite elements with high aspect ratio for dendritic growth of a binary alloy including fluid flow induced by shrinkage, Fluid Dyn. Mater. Proc. 3 (2007) 49–64.
[17] A. Karma, W.-J. Rappel, Phase-field model for computationally efficient modeling of solidification with arbitrary interface kinetics, Phys. Rev. E 53 (1996) R3017–3020.
[18] Y. Sun, C. Beckermann, Diffuse interface modeling of two-phase flows based on averaging: mass and momentum equations, Physica D 198 (2004) 281–308.
[19] Y. Sun, C. Beckermann, A two-phase diffuse-interface model for Hele-Shaw flows with large property contrasts, Physica D 237 (2008) 3089–3098.
[20] X. Tong, C. Beckermann, A. Karma, Q. Li, Phase-field simulations of dendritic crystal growth in a forced flow, Phys. Rev. E 63 (2001) 061601.
[21] J.C. Ramirez, C. Beckermann, A. Karma, H.-J. Diepers, Phase-field modeling of binary alloy solidification with coupled heat and solute diffusion, Phys. Rev. E 69 (2004) 051607.
[22] J.C. Ramirez, C. Beckermann, Examination of binary alloy free dendritic growth theories with a phase-field model, Acta Mater. 53 (2005) 1721–1736.
[23] Y. Lu, C. Beckermann, J.C. Ramirez, Three-dimensional phase-field simulations of the effect of convection on free dendritic growth, J. Cryst. Growth 280 (2005) 320–334.